Interaction between oxygen vacancies on MgO(100)

Fabio Finocchi*
Laboratoire de Physique des Solides, Associé au CNRS, Université Paris-Sud, 91405 Orsay, France

Jacek Goniakowski†
CRMC2-CNRS, Campus de Luminy, 13288 Marseille, France

Claudine Noguera‡
Laboratoire de Physique des Solides, Associé au CNRS, Université Paris-Sud, 91405 Orsay, France
(Received 27 July 1998)

Oxygen-deficient MgO(100) surfaces are studied by means of total-energy calculations, within the density-functional theory. Selected surface configurations presenting increasing densities of neutral oxygen vacancies, ranging from 12.5% to 100%, are considered, the missing oxygen being periodically distributed in the surface layer either homogeneously or in a close-packed fashion. We show that the electronic structure is characterized by occupied states in the gap which result either from the hybridization of atomiclike orbitals localized on vacancy sites, or involve surface magnesium orbitals. The latter case occurs at large vacancy concentrations, and the conditions for the apparition of metallicity in the surface layer are derived. The formation energy of oxygen vacancies is calculated as a function of the vacancy concentration and of the particular configuration. A two-body model potential is proposed to account for their interaction. The activation energy for vacancy diffusion at the surface is also computed, thus providing a complete set of parameters for a description of the thermodynamics as well as of the kinetics of oxygen vacancies on a MgO(100) surface.
[S0163-1829(99)05407-7]

I. INTRODUCTION

In oxide materials, defects are often present, and are responsible for specific optical, transport, magnetic, or catalytic properties.[1–3] The simplest and most often encountered defects are oxygen vacancies which can exist in different charge states, depending upon the oxide and the preparation conditions. When two electrons are trapped in the vacancy, the defect is called an F center, or F_s center if it is localized at the surface.

Oxygen vacancies have been the subject of numerous studies, especially in the bulk of oxides. From calorimetric measurements, formation energies and interaction strengths between vacancies were deduced, using a statistical analysis.[4] In some oxides, e.g., in MgO, electron-spin resonance, optical-absorption, or high-resolution electron-energy-loss experiments[5–7] suggested vacancy clustering. The ordering of cation and oxygen vacancies in nonstoichiometric TiO_x titanium oxides,[8,9] magnesium oxide,[10] or zirconia[11] was characterized, and mechanisms responsible for the ordering were proposed. The transition between an insulating state at low oxygen vacancy concentration and a metallic state at higher concentration was assigned to the overlap between the defect band and the conduction band.[12] From a theoretical point of view, the localization of the excess electron charge has been studied in oxides presenting various degrees of ionicity of the cation-oxygen bond. General agreement exists about the high degree of localization of the F center in MgO,[13,14] while in more covalent titanium, tin, or silicon oxides,[9,15] part of the excess electronic charge is distributed on the neighboring cations.

On surfaces, to our knowledge, there is no experimental determination of the oxygen vacancy formation energy. Calculations generally predict that it is reduced with respect to its bulk value, consistently with the reduced coordination of surface atoms. The interaction between vacancies has been scarcely investigated,[16,17] although it is a major ingredient for understanding the vacancy ordering of defective surfaces upon reconstruction, as observed on many oxide surfaces upon annealing in vacuum. For example, reconstructions were observed on $TiO_2(100)$,[18–21] $TiO_2(110)$,[22,23] $SnO_2(110)$,[24] $SrTiO_3(001)$,[25–27] and α-Al_2O_3 (0001).[28–33] The thermodynamical stability of an ordered configuration is driven by the formation energy of vacancies and their interaction strength. Nevertheless, the observation of ordered configurations of defective surfaces actually relies on the parameters governing vacancy diffusion, such as the activation energy and the temperature.

In this context, we carry out an extensive study of the energetics and of the electronic structure of neutral oxygen vacancies at the (100) surface of magnesium oxide. Such a system can be considered as a prototype for the study of defective oxide surfaces, due to the simplicity of its structure and the large experimental and theoretical knowledge gained in the past years on the ideal surface. Electron-energy-loss-spectroscopy experiments[34] revealed the existence of a surface sensitive feature at 2.3 eV, which was first assigned to an F_s center, but later to a cation vacancy. There is no report of the existence of vacancy ordering leading to surface reconstructions.

From a theoretical point of view, the energetics and electronic characteristics of a single oxygen vacancy were studied by using either semiempirical,[35] or *ab initio*[36,37] Hartree-Fock methods, and density-functional theory (DFT).[14,38] To

our knowledge, only in Ref. 17 were finite concentrations of vacancies in the surface layer explicitly considered and the interaction energy between vacancies derived. The energy to form neutral oxygen vacancies was shown to decrease as a function of the increasing mean density or their proximity, suggesting a tendency toward vacancy clustering. The method used in Ref. 17 is expected to predict qualitative trends correctly, but *quantitative* properties, especially those related to the localization of the excess electrons, are better described by *ab initio* methods.

We thus reconsider the MgO(100) surface in the presence of various mean vacancy concentrations n_F, and, for a given n_F, we simulate different distributions in the surface layer. At $n_F=1$, all the oxygens are removed from the outer layer. This configuration, which is equivalent to a magnesium epitaxial layer on a MgO(100) substrate, is a model system both for highly defective surfaces and for metal-oxide interfaces. By means of total energy calculations, relying on DFT, we compute the electronic structure and the relaxed atomic configurations of the defective surfaces. The detailed analysis of the configurations considered here, allows us to extract basic parameters which can be used to predict the energetics and the electronic structure of any other vacancy distribution. In addition, we calculate the activation energy for the diffusion of a vacancy, thus providing a complete set of parameters for a description of the thermodynamics as well as of the kinetics of oxygen vacancies on an MgO(100) surface.

The paper is organized as follows. In Sec. II we give the computational details. The results for the energetics and the electronic and atomic structures of the selected surface configurations are presented in Sec. III. These are discussed in Sec. IV, and the relevant parameters driving the electronic and energetic characteristics of defective surfaces are derived. Section V is devoted to an analysis of the diffusion of an oxygen vacancy in the surface layer.

II. COMPUTATIONAL DETAILS

Total-energy calculations are performed in the framework of DFT within the local-density approximation (LDA) for the exchange and correlation energy. The interaction between core ($1s$ atomic states for oxygen, and $1s$, $2s$, and $2p$ states for magnesium) and valence electrons is described by norm-conserving pseudopotentials in the Kleinman-Bylander form[39] including *s*, *p*, and *d* components for oxygen, and *s* and *p* components for magnesium. A local reference potential is chosen (a *d* component for oxygen, and an *s* component for magnesium). We follow the prescriptions given by Troullier and Martins[40] for the generation of oxygen and magnesium pseudopotentials to obtain an optimal total-energy convergence as a function of the size of the basis set. The core radii chosen for oxygen are 1.38, 1.75, and 1.38 a.u. for the *s*, *p*, and *d* components, respectively. The core radii for magnesium are 2.0 a.u. for both *s* and *p* components. The oxygen pseudo-potential was already used in a previous study of Li_nO_m clusters.[41] The electronic states are expanded in a plane-wave basis set. An energy cutoff of 44 Ry gives total energies converged within 0.1 eV per formula unit.

We use a slab geometry to represent the nonstoichiometric surfaces, with a surface unit cell $(2\sqrt{2}\times 2\sqrt{2})R45°$ containing eight MgO formula units. Due to the large size of the supercell, the Γ point only has been considered for the integration of the electronic density in the two-dimensional Brillouin zone (BZ). With such a choice, a difference of 0.06 eV in the surface energy of the unrelaxed slab is obtained with respect to a fully converged calculation using ten special **k** points[42] in the irreducible part of the BZ corresponding to the $(\sqrt{2}\times\sqrt{2})R45°$ surface unit cell. The slab is four layers thick. A preliminary calculation with no vacuum between the repeated slabs allows us to check the accuracy of the method on bulk properties. We find an equilibrium lattice constant a_0, a bulk modulus B_0, and a cohesion energy E_{coh} equal to $a_0=4.24$ (4.2) Å, $B_0=0.94$ (0.95) eV/Å^3, and $E_{coh}=11.2$ (10.3) eV per formula unit relative to the neutral atoms, respectively. These values present deviations from the experimental ones, written in brackets, which are typical of this kind of approach.

The surface calculations are performed by introducing a vacuum region of four MgO layers thickness between two repeated slabs in the direction perpendicular to the surface. We check that the two layers at the bottom of the slab are negligibly modified when oxygens are removed from the top layer. A full geometry optimization of the three topmost MgO layers is performed in order to determine the equilibrium geometry of each surface configuration. The search for the energy minimum is stopped when atomic forces are less than 0.01 eV/Å.

Actually, two methods are currently used to simulate a defective system. Either the defect is introduced in the middle of an embedded cluster, or a supercell geometry is used, in which the defect is periodically repeated. For instance, the DFT calculation made in Ref. 14 actually accounts for a finite concentration (25%) of homogeneously distributed vacancies. Since here we aim at considering nonzero concentrations n_F of vacancies, we use the supercell geometry previously described, with $n_F=12.5\%$, 25%, 50%, and 100%. This amounts to removing one, two, four, and eight neutral oxygen atoms per unit cell in the surface top layer (Fig. 1), respectively. For the two intermediate concentrations (25% and 50%), we simulate two distributions of vacancies: the first one, which is homogeneous, and another configuration in which the vacancies are close packed [denoted as (*h*) and (cp) in Fig. 1 and in the following, respectively]. The four surfaces with homogeneously distributed vacancies correspond to ordered configurations with $(2\sqrt{2}\times 2\sqrt{2})R45°$, 2×2, $(\sqrt{2}\times\sqrt{2})R45°$, and 1×1 primitive unit cells, respectively.[43]

In the case of highly defective surfaces, we complement the results obtained with the method previously described, by means of a band structure calculation performed within the Full-potential linear-muffin-tin-orbital method (FP-LMTO),[44] with the same exchange and correlation LDA functional. The calculation is performed on a four-layer-thick slab with two identical terminations. A primitive 1×1 surface unit cell is assumed, and 13 **k** points are used for integration of electronic density in the irreducible part of the two-dimensional (2D) Brillouin zone for the fully defective surface, while a $(2\sqrt{2}\times 2\sqrt{2})R45°$ unit cell and six **k** points were used at concentration $n_F=50\%$ (cp).

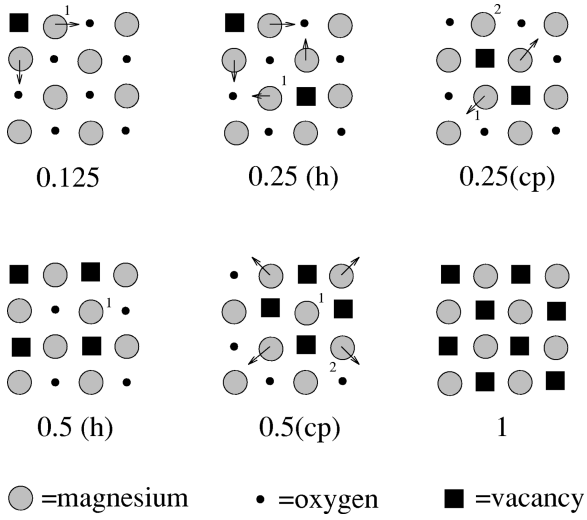

FIG. 1. Schematic top view of the surface configurations with 12.5%, 25%, 50%, and 100% concentrations of neutral oxygen vacancies. *h* and cp refer to homogeneous or close-packed configurations of vacancies, respectively. The inequivalent magnesiums which are noticeably displaced when oxygens are removed (arrows indicate the directions of their horizontal displacements) have been labeled for the sake of discussion.

III. DESCRIPTION OF NONSTOICHIOMETRIC SURFACES

A. Atomic structure

On the stoichiometric surface, the ground-state atomic configuration that we find is in agreement with previous calculations or experimental findings. The outer interplane distance is slightly contracted, with an inward relaxation of 0.6%. The rumpling amounts to 3.6%, with the oxygen atoms pushed outwards. Recent grazing-incidence x-ray scattering experiments[45] performed on high-quality surfaces yield values of $0.56\% \pm 0.35\%$ and $1\% \pm 0.5\%$, while recent quantitative low-energy electron-diffraction analysis[46] yields 0.2% and 3.3% for these two quantities, respectively.

The removal of oxygen atoms results in a large relaxation of the surface atoms both in the surface plane and along the perpendicular direction. In Table I, we give the relative displacements $\delta d_{\parallel}/d_0$ of the neighboring magnesiums in the surface layer, normalized to the bulk interatomic distance d_0, and the relative change $\delta d_{\perp}/d_0$ in the interplane Mg-O distance. It should be noted that $\delta d_{\parallel}/d_0$ vanishes by symmetry for configurations with 50% (*h*) and 100% concentrations. For all the surface configurations that we consider, $\delta d_{\parallel}/d_0$ and $\delta d_{\perp}/d_0$ turn out to be positive, which indicates displacements away from the vacancy in the surface layer and a weakening of the interplane Mg-O bond. The first effect results from the bond breaking upon the creation of the vacancy. A contraction of the remaining surface Mg-O bonds results, which fulfills the general trend that the smaller the coordination, the shorter the bond.[3] The weakening of interplane Mg-O bonds, on the other hand, is due to the redistribution of the excess electrons, which results in a charge decrease on the subsurface oxygens—due to an antibonding hybridization of the oxygen orbitals with the F_s state—and to a lesser extent on the surface magnesiums.

For the smallest concentration of vacancies, we find an outward displacement of the surface magnesiums in the surface layer of 0.06 Å and a very small inward relaxation (0.01 Å) of the neighboring oxygen, with respect to the vacancy position. Our values are of the same order as those obtained for a single vacancy in an embedded cluster, by an *ab initio* Hartree-Fock method[36] (0.04 and 0.04 Å , respectively). For a concentration equal to 25% (*h*), our results are in excellent agreement with those of Ref. 14, including the displacement of 0.06 Å of the magnesium below the vacancy which moves away from the vacancy (0.05 Å in Ref. 14). While there is no evidence of monotonic variations of $\delta d_{\parallel}/d_0$ as a function of the vacancy concentration n_F, the dilation of the interplanar Mg-O distance $\delta d_{\perp}$ keeps increasing with n_F.

B. Vacancy formation energy

We define the energy of formation of a neutral oxygen vacancy $E_{form}(N,i)$ in a system containing N F_s centers per unit cell in a configuration i ($i=h$,cp) as follows:

$$E_{form}(N,i)=\frac{E(0)-E(N,i)-NE_{\mathrm{O}}}{N}, \tag{1}$$

where the computed total energies of the stoichiometric slab $E(0)$ and of the slab containing N oxygen vacancies per unit cell in the ith configuration $E(N,i)$ include atomic relaxations but do not take into account zero-point energies. The total energy of the isolated oxygen pseudoatom E_{O} is computed for the spin-polarized configuration $(2s)^{\uparrow\downarrow}(2p)^{\uparrow\uparrow\uparrow}$ in the local-spin-density approximation. The imprecision of the computed formation energy introduced by the Γ-point sampling is estimated to be $\simeq 0.1$ eV, as checked on the n_F

TABLE I. Relative displacements of surface magnesiums $\delta d_{\parallel}/d_0$ in the surface layer and relative change $\delta d_{\perp}/d_0$ in the interplane Mg-O distance, normalized to the bulk Mg-O interatomic distance d_0. Inequivalent magnesiums are labeled according to Fig. 1; (*h*) and (cp) refer to homogeneous or close-packed configurations of vacancies, respectively.

Concentration	$\delta d_{\parallel}/d_0$	$\delta d_{\perp}/d_0$
12.5%	Mg_1: +3.0%	Mg_1: +1.7%
25% (*h*)	Mg_1: +1.3%	Mg_1: +2.0%
25% (cp)	Mg_1: +1.8%; Mg_2: +1%	Mg_1: +2.3%; Mg_2: +2.2%
50% (*h*)	Mg_1: 0%	Mg_1: +3.4%
50% (cp)	Mg_1: 0; Mg_2: +3.2%	Mg_1: +6.5%; Mg_2: +3.6%
100%	0%	+9%

TABLE II. Formation energies $E_{form}(N,i)$ per neutral oxygen vacancy (in eV). N is the number of vacancies per unit cell and i ($=h$ or cp) refers to the distribution of vacancies.

N	n_F	$E_{form}(N,h)$ (eV)	$E_{form}(N,\mathrm{cp})$ (eV)
1	12.5%	9.8	
2	25%	10.2	10.2
4	50%	10.4	10.2
8	100%	9.8	

$=50\%$ (h) configuration.[47] From a knowledge of $E_{form}(N,i)$, as defined in Eq. (1), the thermodynamically stable configuration of a surface in contact with any oxygen reservoir (consisting of oxygen atoms or molecules according to the experimental conditions) may be easily derived.

Table II gives the values of $E_{form}(N,i)$ that we obtain. In all cases, the reduction of $E_{form}(N,i)$ due to relaxation effects is less than 0.1 eV. The value $E_{form}(1)=9.8$ eV that we find for a single vacancy in the supercell is in excellent agreement with previous calculations: 9.35 eV in Ref. 37 using the Hartree-Fock method plus correlation, and polarization corrections on an embedded cluster. The use of an Hartree-Fock method without corrections gives a much smaller value: 7.7 eV in Ref. 36. Our computed $E_{form}(1)$ at the surface is about 1 eV smaller than in the bulk,[14] consistent with the smaller number of broken bonds when removing a surface oxygen. E_{form} gently grows as a function of n_F, up to $n_F=50\%$. Our result $E_{form}(2;h)=10.2$ eV($n_F=25\%$) can be compared with the value $E_{form}(2,h)=9.77$ eV given in Ref. 14, using the plane-wave pseudopotential approach.

The energy needed to remove oxygens may be thought as including the intrinsic contribution of an isolated vacancy in the limit $n_F\rightarrow 0$, and terms due to the interaction between neighboring vacancies, which depend upon both n_F and the actual vacancy configuration. The increase of $E_{form}(N,h)$ that we find up to $n_F=50\%$ is the signature of a small effective repulsion between neighboring vacancies. However, at constant n_F, for both 25% and 50% concentrations, a few tenths of an eV are gained when vacancies are close packed rather than homogeneously distributed. A possible explanation for this apparent contradiction will be given in Sec. IV.

C. Electronic structure: hybridized vacancy states

The electronic structure of stoichiometric MgO consists of a filled valence band, of mainly oxygen character, and an empty conduction band built mainly from magnesium states. Upon removal of neutral oxygens, states disappear in the valence band, and the two electrons left by each missing oxygen are accommodated in quantum states whose energy generally lies in the bulk band gap. Since a single **k** point is used for the Brillouin-zone sampling, we obtain as many filled gap states as vacancies in the unit cell. In Fig. 2 we report the energy of these F_s states with respect to the top of the valence band maximum (VBM), up to $n_F=50\%$. The use of such a reference to specify the energy of the defect states avoids the well known drawback of DFT-LDA calculations, in which the highest occupied molecular orbital–lowest unoccupied molecular orbital gap is systematically underestimated. Here we find a gap of 5.7 eV, to be compared to the experimental value 7.8 eV, and to a DFT-LDA value of 5.2 eV obtained for bulk MgO by using the same pseudopotentials and a well-converged sampling of the Brillouin zone.

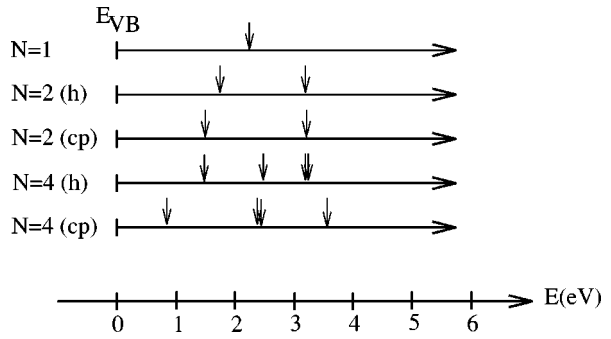

FIG. 2. Energy levels of the filled defect states in the gap, for the different surface configurations. The tops of the bulk valence bands E_{VB} have been aligned.

For the smallest vacancy concentration, the F_s center is located at 2.24 eV above the valence-band maximum. The interaction between vacancies originates an F_s band, whose width increases with their concentration n_F, still depending on their spatial distribution. In the Hartree-Fock calculations on embedded clusters containing a single vacancy, the F_s center was found at 4.6 eV (Ref. 37) or at about 7 eV (Ref. 36) (i.e., halfway between the valence-band maximum and the bottom of the Hartree-Fock conduction band) above the VBM. For an homogeneous concentration of 25% of vacancies, the authors of Ref. 14 found it at 2.3 eV. Since they used the lowest-order Monkhorst-Pack scheme for the generation of special **k** points used in the BZ integration, they obtained a single peak at the center of gravity of the vacancy band. Its position is consistent with our findings, which give the extrema of this band at 1.72 and 3.2 eV above the VBM, respectively. When a restricted basis set is used, with no floating orbitals at the vacancy sites, the F_s center lies higher in the gap, at about 2 eV below the bottom of the conduction band.[17]

The degree of localization of the excess electrons in the jth defect state is better visualized by plotting the surfaces of equal electron density $|\psi_j(\vec{r})|^2=\mathrm{const}$. In the case of a single vacancy we find a high degree of localization of the electrons in the vacancy site, in agreement with most authors. The two electrons are trapped by the positive electrostatic potential exerted by the neighboring magnesiums, which is high in such an ionic material. The F_s center may thus be thought of as a kind of ''vacancy orbital'' localized at the vacancy site.

Figures 3(a) and 3(b) represent isodensity plots for the two gap states associated with a 25% concentration of vacancies in a close packed configuration. For the lower-energy state [Fig. 3(a)], the electronic density is enhanced between the two vacancies. For the state at higher energy [Fig. 3(b)], a two-lobe-like density is found, with a nodal surface separating the vacancy sites. These are the signatures of bonding and antibonding states formed by hybridization between the two vacancy orbitals. Some small hybridization of antibonding character with the s or p orbitals of oxygen (at the surface

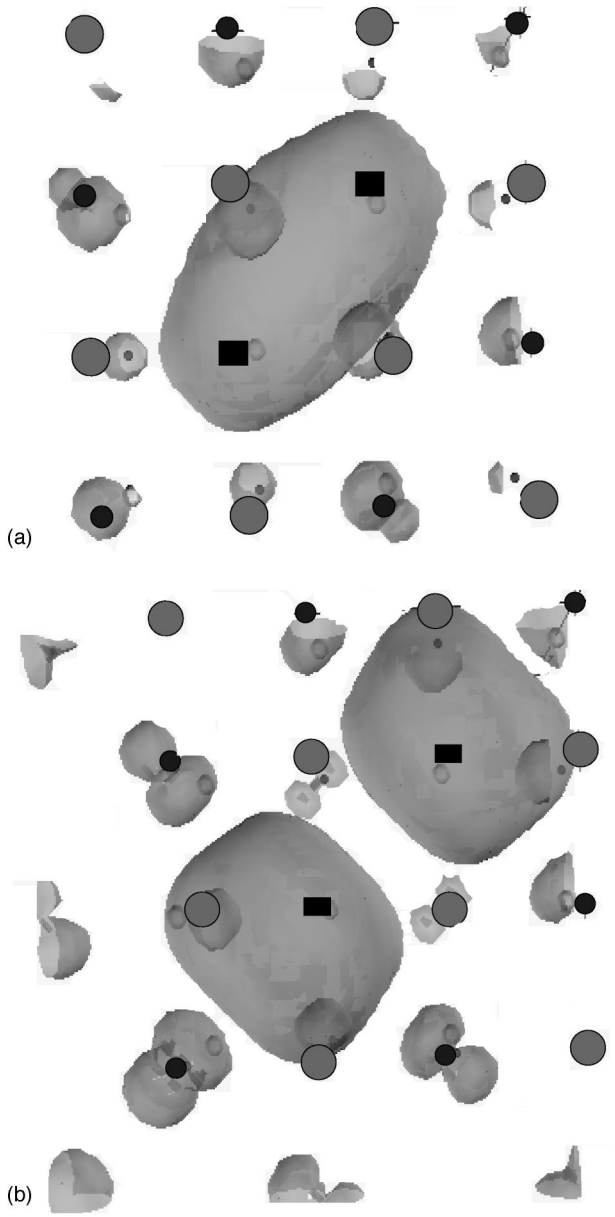

FIG. 3. Isodensity surfaces (about 15% of maximum density) for the two gap states associated with a 25% concentration of vacancies in a close-packed configuration. (a) On the left: the bonding state. (b) On the right: the antibonding state (see text). A top view of the surface is presented with oxygen atoms as black dots and magnesiums as light spheres. The location of the vacancies is indicated by black boxes.

or in the layer beneath) may also be recognized in Fig. 3. This results mainly from the orthogonality of the gap states to the valence-band states.

A similar hybridization is actually found on all the defective surfaces that we consider. As discussed further in Sec. IV, the hybridization between vacancy orbitals is one of the key factors determining the overall character (either insulating or metallic) of the electronic structure of the defective surfaces.

D. Metallic character of highly defective surfaces

We first discuss the ordered 1×1 vacancy configuration for the fully defective surface, which can be considered as a

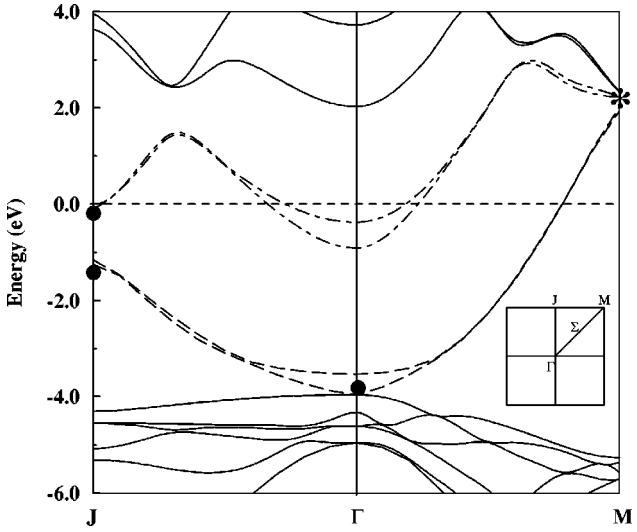

FIG. 4. Band structure of the fully defective (1×1) surface along the three symmetry lines J-Γ-M of the 2D Brillouin zone (inset), as obtained through the FP-LMTO calculation. The dashed horizontal line represents the Fermi level, and black dots (star) indicate the energy positions of the filled (empty) Bloch states at Γ calculated in the large supercell. The two bands in the gap of the projected bulk band structure are represented by dashed and dash-dotted lines.

prototype of a planar metal-oxide interface. The analysis of its electronic structure may help in understanding the relation between strongly defective oxide surfaces and metal overlayers grown on their own oxide. Although the thermodynamically stable state of such a defective surface might consist of Mg clusters on MgO(100),[48] the present study is relevant for a metastable epitaxial growth during the first stages of deposition of Mg onto MgO(100) at temperatures low enough to prevent atomic diffusion.

There are several indications that the fully defective surface presents some features which are *qualitatively* different from those occurring at low vacancy concentrations. For example, extrapolating the trend found for the concentration dependence of the vacancy formation energy (Sec. III B), a value larger than 10.4 eV for $E_{form}(8)$ would be predicted. However, we find $E_{form}(8)=9.8$ eV. In addition, the analysis of the charge density maps reveals that only seven upon the eight filled gap states display the characteristics of hybridized vacancy orbitals. The eighth one, just below the Fermi level E_F, shows density maxima on top of the surface magnesiums, and its symmetry is inconsistent with that of a totally antibonding state built from vacancy orbitals. The totally antibonding state is actually found at higher energies, about 2.3 eV above E_F.

In order to obtain more insight into the electronic structure of this surface, we have performed separately an accurate band structure calculation of the slab with a primitive 1×1 unit cell, using the FP-LMTO method. The results along the high symmetry lines J-Γ-M are shown in Fig. 4. In the energy ranges $E<-4.0$ eV and $E>2.5$ eV, are located the valence and the conduction bands, respectively. In the gap region[49] $-4.0<E<2.5$ eV, two bands are found (drawn in dashed and dash-dotted lines in Fig. 4), which are doubly degenerate apart from a small region around the Γ point. The degeneracy originates from the symmetry be-

tween the top and bottom faces, and reveals the existence of a small residual interaction between the two terminations, which, in any case, does not modify our conclusions. One of the two bands lying in the gap starts at the top of the valence band at Γ and extends up to the bottom of the bulk conduction band at M. The second one starts at $E \approx -0.5$ eV at Γ and is clearly hybridized with the conduction band both along J-Γ and Γ-M directions. In Fig. 4 we report, as black dots, the energy of the gap states found at Γ in the supercell calculation, i.e., at the high-symmetry point Γ, J, M, and Σ [Fig. 4(b)], of the Brillouin zone of the 1×1 surface. The two calculations are in excellent agreement, aside from the position of the last filled gap state, which is predicted at Γ in the FP-LMTO calculation and at J in the pseudopotential approach. Actually, this amounts to a very small energy difference of 0.4 eV. The agreement is also excellent as far as the empty vacancy orbital state of fully antibonding character (at M) is concerned (star in Fig. 4).

With the help of the charge-density analysis, we can assign a different origin to the two gap bands: the most dispersive one (dashed line in Fig. 4) results from the hybridization of vacancy orbitals (the F_s band, as introduced in Sec. III C). At Γ the states are fully bonding, and at M they are fully antibonding. Remarkably, the vacancy orbitals keep a strong identity even on the fully defective surface. The second gap band (dash-dotted line in Fig. 4) involves states which are localized on the surface magnesiums. This band may be called a surface conduction band (Mg_s band): it is shifted toward lower energies, with respect to the bulk conduction band. The Fermi level intercepts the two bands, conferring a metallic character to the surface.

We perform a similar analysis for the surface with $n_F = 50\%$ in a close-packed (cp) configuration. As on the fully defective surface, the configuration with $n_F = 50\%$ (cp) involves magnesiums surrounded by four oxygen vacancies. On the oxygen sublattice, each vacancy has two vacancies in its first coordination shell. The FP-LMTO band structure, corresponding to the the $(2\sqrt{2}\times2\sqrt{2})R45°$ unit cell, is shown in Fig. 5. The top of the valence band lies close to -3.5 eV, while several surface conduction bands may be recognized above -0.2 eV. The four inequivalent vacancies in the unit cell give rise to four bands, among which one is in the range -3.5–-2.5 eV, two are located between -2.0 and -1.0 eV, and the fourth one is hybridized with the surface conduction band (see Fig. 5). On average, each vacancy band disperses less than 0.5 eV, but their overall width amounts to 4 eV. The bands located between -0.5 eV and the bottom of the bulk conduction band (above 1.0 eV, not shown in Fig. 5) originate from surface magnesium states, which are pushed toward lower energies with respect to the bulk ones. Both for $n_F = 50\%$ (cp) and for $n_F = 100\%$, the Mg states are highly hybridized either with states of other inequivalent surface magnesiums, or with bulk magnesium states, as a result of the small Mg-Mg distance in MgO (2.96 Å versus 3.21 Å in bulk Mg). The Fermi level intercepts the highest vacancy band and the surface conduction bands, conferring a metallic character to the surface.

These findings show that the *nature* of the filled gap states varies with the vacancy concentration and configuration, and that only a good spanning of space by the basis vectors on which the wave functions are expanded permits one to obtain a reliable description. One has to be very careful when using atomic or localized orbitals as in semiempirical approaches or in some *ab initio* methods. For instance, in the semiempirical Hartree-Fock approach used in Ref. 17, the excess electrons trapped by the vacancies could only be accommodated on the neighboring magnesium orbitals. An overestimate of the quadrupolar moment of the defect charge resulted, which yielded a strong attraction between vacancies and incorrectly predicted a desorption of neutral magnesiums.

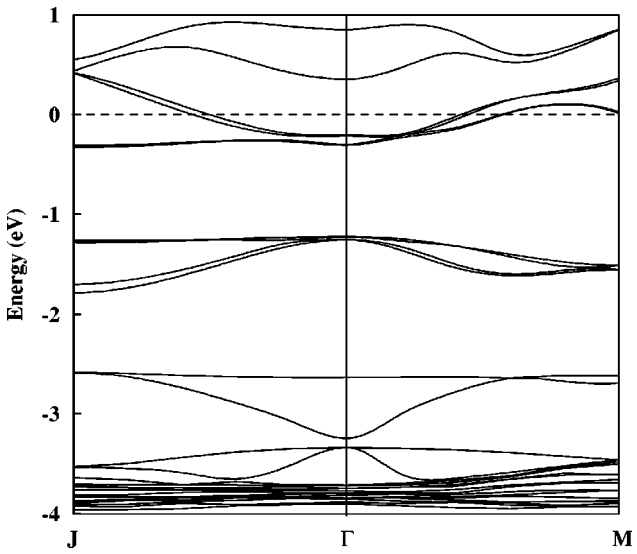

FIG. 5. Band structure of the $(2\sqrt{2}\times2\sqrt{2})R45°$ surface with a $c = 50\%$ (cp) vacancy density along the symmetry lines J-Γ-M. The dashed horizontal line represents the Fermi level.

IV. THEORETICAL ANALYSIS

From these results, parameters governing the electronic structure and the energetics of nonstoichiometric MgO(100) surfaces may be derived. We successively consider the hybridization between vacancy orbitals, the strength of the interaction between vacancies, and the transition toward metallicity.

A. F_s center hybridization

The charge-density maps, shown in Fig. 3, confirm that, for all the surfaces that we consider, there exist gap states (or bands) which result from the hybridization between vacancy orbitals. In this section, we thus try to interpret the energy positions of such states within a simple tight-binding model. A Hamiltonian matrix is constructed using a basis of vacancy orbitals. Its diagonal elements ϵ_0 are the effective energies of the atomic-like orbitals and the nondiagonal elements β_n are the resonance integrals associated with electron hopping between vacancies in position of nth neighbor on the oxygen sublattice. The model takes into account the full two-dimensional periodicity of the surface layer. In principle, it can include overlap integrals S_n, but, for the sake of simplicity, here we assume that $S_n = 0$, for all values of n.

Starting from the eigenvalues computed within the LDA, we deduce β_n for $(n<4)$ and ϵ_0 for the different configurations studied. The results are given in Table III. The effective

TABLE III. Analytical expressions for the energy levels of the gap states at Γ, within the tight-binding model (see text), for the different concentrations and distributions of vacancies. The right column gives the values of ϵ_0 (with respect to the VBM) and of β_n (in eV) which best fit the numerical results for the relaxed surfaces.

Concentration	Eigenstate expressions	ϵ_0	β_1	β_2	β_3
$c=12.5\%$	$\epsilon=\epsilon_0$	2.24			
$c=25\%$ (h)	$\epsilon=\epsilon_0+4\beta_3$ $\epsilon=\epsilon_0-4\beta_3$	2.46			-.18
$c=25\%$ (cp)	$\epsilon=\epsilon_0+\beta_1$ $\epsilon=\epsilon_0-\beta_1$	2.36	-.86		
$c=50\%$ (h)	$\epsilon=\epsilon_0+4\beta_2+4\beta_3$ $\epsilon=\epsilon_0-4\beta_2+4\beta_3$ $\epsilon=\epsilon_0-4\beta_3(\times 2)$	2.57		-.12	-.16
$c=50\%$ (cp)	$\epsilon=\epsilon_0+2\beta_1+2\beta_2$ $\epsilon=\epsilon_0-2\beta_2(\times 2)$ $\epsilon=\epsilon_0-2\beta_1+2\beta_2$	2.28	-.70	-0.04	
$c=100\%$	$\epsilon=\epsilon_0+4\beta_1+4\beta_2+4\beta_3$ $\epsilon=\epsilon_0-4\beta_3(\times 4)$ $\epsilon=\epsilon_0-4\beta_2+4\beta_3$ $\epsilon=\epsilon_0-4\beta_1+4\beta_2+4\beta_3$	1.16	-.73	+0.07	+.16

vacancy orbital energy ϵ_0 is nearly constant on all surfaces, except on the fully defective one, due to the presence of excess electrons on the surface magnesiums, as previously noted. The resonance integral β_1 between first neighbors is rather large, lying in the range -0.7–-0.8 eV. Interestingly, we find a nonmonotonic evolution for β_n as a function of n, although the distance between two vacancies increases with n. One may thus conjecture that the resonance integrals, in this simple model, do not represent direct hopping processes for the electrons in the surface layer. From an examination of Fig. 1, one may indeed see that hopping is mediated by magnesium atoms for $n=2$ and by oxygen atoms for third neighbors ($n=3$). The oxygen-mediated hopping is also apparent in Fig. 3. This remark helps us to understand the large discrepancy between the values of β_3 deduced from surfaces at low n_F ($\beta_3\approx -0.17$ eV) and that obtained for the fully defective surface ($\beta_3=+0.17$ eV). Indeed, for $n_F=100\%$, no oxygen is left in the surface layer, so that hopping can only be mediated by oxygens beneath the surface plane.

From this model, the overall width W of the vacancy bands can be predicted for any defective surface. W is determined by the energy difference between the most bonding and the most antibonding states, which can be constructed from vacancy orbitals. It is basically governed by the local environment of the most close-packed vacancies. If the latters have Z_{n_0} closest vacancies in position of n_0th neighbors, then $W\approx 2Z_{n_0}\beta_{n_0}$. In the selected configurations that we study, the largest band widths are found for $n_F=50\%$ (cp) and $n_F=100\%$. They amount approximately to $4|\beta_1|$ and $8|\beta_1|$.

B. Interaction between oxygen vacancies

The energetics of defective surfaces can be completely characterized by giving the formation energy of an isolated vacancy E_0 (in the limit $n_F\rightarrow 0$) and the interaction energies between vacancies, as a function of their positions. As a first approximation, one may represent the latter by distance-dependent pairwise terms u_n for vacancies in position of nth neighbors. The energy of formation of a vacancy $E_{form}(N,i)$, in a system containing N F_s centers per unit cell in a configuration i ($i=h$,cp), is expressed as a function of E_0 and the u_n as follows:

$$E_{form}(N,i)=E_0+\frac{1}{2}\sum_n Z_n u_n, \tag{2}$$

where Z_n is the number of vacancies in the nth coordination shell of a given vacancy site. By calculating differences of $E_{form}(N,i)$, one can eliminate the intrinsic term E_0 and most of the long-distance interactions ($n>4$), and deduce the values of u_n. For instance, apart from terms u_n with $n>4$, $E_{form}(2,h)-E_{form}(1)=2u_3$ and $E_{form}(2,cp)-E_{form}(1)=u_1/2$. Using the data of Table II, we find

$$u_1=0.8 \text{ eV}, \quad u_2=0.1 \text{ eV}, \quad u_3=0.2 \text{ eV}.$$

The interaction potentials u_n are all positive, indicating a repulsion between vacancies. In all cases, they are small with respect to the energy E_0 needed to create an isolated vacancy ($E_0\approx 10$ eV), similarly to what was found in nonstoichiometric titanium oxides ($E_{form}=4.47$ eV; $u_1=0.236$ eV).[4] The positive u_n values result from the repulsion between localized wave functions; they are small mainly because of the neutrality of the defect. The nonmonotonic variation of u_n with n correlates with that of the effective resonance integrals discussed above.

At $n_F=25\%$, the stabilization of a few tenths of an eV obtained when vacancies are close packed rather than homogeneously distributed comes from a subtle competition between the strength and the number of interactions: the repulsion u_1 is stronger in the close-packed configuration, but it is counted only once ($u_1<4u_3$).

This analysis yields consistent interaction energies u_n when the excess electron distribution is well localized on the vacancy sites. On the fully defective surface and on the surface with $n_F=50\%$ (cp), since the Fermi level intercepts the surface conduction band(s), a nonnegligible part of the excess electron density is distributed on the surface magnesiums. The interaction between vacancies can no longer be predicted with the u_n values given above.

C. Transition toward metallicity

The analysis of the electronic structure of defective MgO surfaces shows that there are two kinds of quantum states, which are in competition to accommodate the excess electrons left by the missing oxygens. At very low concentration of vacancies ($n_F=12.5\%$), the electrons are trapped into the vacancy orbitals, whose energy lies in the gap. These orbitals are little hybridized, because the distance between the vacancies is much larger than the typical radius of the vacancy state. A very narrow band is formed. This band is entirely located within the surface band gap, so that it is completely filled and the surface conduction band is empty. The surface is insulating.

When the density of vacancy increases, the surface conduction band involves orbitals located on strongly inequivalent magnesium sites. Despite this fact, the minimum of the surface conduction band Mg_s does not shift appreciably as a function of n_F. This is likely due to the fact that the two electrons trapped on each vacancy site mimic quite well the missing oxygens, at least as far as the Madelung potential acting on the magnesiums is concerned, and to the fact that the sp band width resulting from magnesium-magnesium hybridization is quite wide. As a consequence, despite the increase of the vacancy orbital bandwidth W (Sec. IV A), the vacancy F_s band(s) and the surface conduction band(s) Mg_s do not overlap. The surface remains insulating, since the vacancy orbital bands can accommodate exactly all the excess electrons left behind by the missing oxygens. This situation occurs for $n_F=25\%$ (h), $n_F=25\%$ (cp), and $n_F=50\%$ (h).

In our calculation, the surface with $n_F=50\%$ (cp) is the critical configuration at which the two bands start to overlap, since the energy difference between the top of the valence band and the bottom of the Mg_s band is of the order of W. For this configuration, and at higher vacancy concentrations, the F_s band and the Mg_s band overlap and are partially filled, conferring a metallic character to the surface. When metallicity occurs, the energetics of the vacancies, and in particular their effective interactions, are modified (Sec. IV B). The filled gap states belong either to the F_s or the Mg_s band, and their degree of localization varies accordingly.

The criterion for having a metallic surface thus relies on a comparison between the vacancy orbital band width W and the surface band gap. While one may be confident that a good estimate of W as a function of concentration and surface configuration has been obtained within the computational framework used here, the same is not true regarding the surface band gap, due to the well-known underestimate of gap widths by DFT methods.[50] In our calculation, the bulk band gap is equal to $G_B=5.2$ eV and the surface band gap is of the order of $G_S=3.7$ eV. Experimentally, on the other hand, $G_B=7.8$ eV and $G_S=6.3$ eV.[51,52] Although the difference G_B-G_S is correctly accounted for, the absolute values of the gaps are not well reproduced. It is thus likely that the transition toward metallicity should occur at larger concentrations or for more closely packed configurations than $n_F=50\%$ (cp). Since the largest F_s bandwidth that can be achieved is $W=8|\beta_1|$ ($n_0=1$ and $Z_{n_0}=4$ in the expression $W=2Z_{n_0}\beta_{n_0}$), which is of the order of the experimental value of G_S, we expect the surface to be metallic whenever at least one vacancy is surrounded by four others in position of first neighbors on the surface oxygen sublattice. This is obviously the case when all the oxygens are missing in the surface layer ($n_F=1$), as found in our calculation.

V. DIFFUSION OF A NEUTRAL OXYGEN VACANCY ON MgO(100)

The energy stabilization found when the oxygen vacancies are in a close-packed arrangement rather than homogeneously distributed can lead to vacancy clustering in actual experiments, provided that diffusion processes are efficient enough. It is thus of interest to derive the parameters governing the diffusion of a neutral oxygen vacancy.

By using the same large unit cell as before and simulating a concentration $n_F=12.5\%$, we calculate the barrier height that an oxygen atom has to overcome to fill the vacancy site. For symmetry reasons, the saddle point is located at middistance between the two extremities of the diffusion path (indicated by a dashed line in Fig. 6), but its position z in the direction perpendicular to the surface is *a priori* unknown. The diffusing oxygen atom may pass above or below the surface top layer. By performing a full geometry optimization, we find that diffusion takes place *above* the top layer, that is, there is a single energy minimum as a function of z. At the saddle point, the diffusing oxygen is at equal distance $d_1=1.81$ Å between two magnesiums. The latters are pushed laterally from their original positions, together with their neighboring oxygens. Contractions of the Mg-O interatomic distances d_2 and d_3 result ($d_2=1.94$ Å, $d_3=2.11$ Å). A residual stress remains at the edge of the unit cell, which could, in principle, be removed by using a larger unit cell.

From an electronic point of view, the saddle point configuration is characterized by a filled state located at 2.35 eV above the top of the valence band (to be compared to 2.24 eV when the diffusing atom is at a lattice site). The electron distribution associated with this state is shown in Fig. 6(b). It presents two main lobes located at the two extremities of the diffusion path and some antibonding contribution on the diffusing atom. The two oxygen lattice sites represent attractive regions for the electrons, which are equally shared between them for symmetry reasons. It should be noted again that the use of a plane-wave basis to expand the orbitals is very convenient for a description of such a complex process, since no

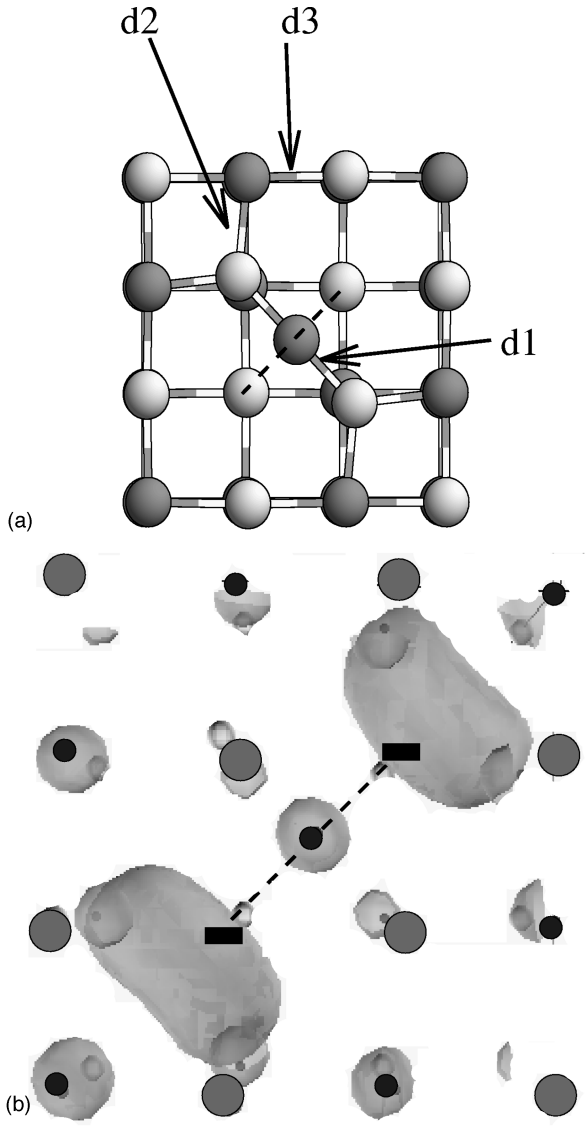

FIG. 6. Characteristics of the saddle point in the diffusion path of an oxygen vacancy on MgO(100). (a) Atomic configuration. (b) Isodensity surface for the vacancy gap state, plotted at about 15% of the maximum state density. The diffusion path is drawn as a thick dotted line.

assumption about the spatial behavior of the wave function has to be made at the beginning of the calculation, as is the case when localized bases are used.

The activation energy for the diffusion of the vacancy E_a is equal to the energy difference between the two surface configurations with the diffusing oxygen at its lattice site or at the saddle point. In the bulk, we are aware of two experimental determinations of E_a which give, respectively, $E_a = 2.21$ eV (Ref. 53) and 1.1 eV.[54] To our knowledge, there is no measurement on the (100) surface. Recently, E_a has been calculated by a semiempirical method, for both neutral and charged vacancies in bulk MgO.[55] For neutral vacancies the authors of Ref. 55 found $E_a = 3.13$ eV. At the surface, we find a value of E_a equal to 2.6 eV. This value seems slightly overestimated, since, in the bulk, E_a does not exceed 2.2 eV and since it should be lower at the surface. We have considered several factors which could affect the value of E_a. First, we have tried to improve the magnesium pseudopotential by adding a *d* component to Mg. We have chosen a *p* local reference potential and a *d* core radius equal to 2 a.u. After computing the fully relaxed state for the two vacancy configurations with this pseudopotential, we find that the height of the diffusion barrier is lowered, down to a value of 2.1 eV, while the atomic arrangement and the electronic structure are essentially unchanged. This substantial decrease of E_a is likely due to the strongly anisotropic environment of the surface magnesiums close to the diffusion path, which enhances the need for *d*-symmetry orbitals. We have also checked that the *a posteriori* treatment of valence electrons by a generalized gradient approximation[56] (GGA) rather than a local density approximation for exchange and correlation does not substantially modify our computed E_a more than few tens of meV.[57]

We therefore conclude that the barrier height for oxygen diffusion at the surface layer is equal to about 2 eV. The saddle point is located above the surface, at middistance between two lattice sites, on which the two excess electron are equally shared.

VI. CONCLUSION

We have performed an extensive study of formation energy, interaction and diffusion of neutral oxygen vacancies on the MgO(100) surface. We have considered selected periodic arrangements of vacancies, with several concentrations n_F; for two intermediate values of n_F, we have simulated configurations in which the missing oxygens are distributed either homogeneously or in a close-packed fashion in the unit cell. Those selected configurations have allowed us to extract the basic parameters which drive the energetics and the electronic structure of defective surfaces, and which can be used to predict the behavior of specific surface configurations found experimentally.

The energy needed to remove a neutral oxygen atom is close to 10 eV, in agreement with previous estimates. Up to a critical concentration, which is about 50% according to our calculations, the interaction between vacancies is repulsive and of the order of a few tenths of an eV. This can, however, favor some close-packed configurations, depending on the detailed counting of the repulsive interactions.

The surface electronic structure presents two types of bands in the gap of the projected bulk band structure. One is due to the hybridization of atomic-like states localized at the vacancy sites (''vacancy orbitals''). The other is mainly built from surface magnesium states.

For high vacancy concentrations and/or for close-packed configurations, the vacancy band width exceeds the surface band gap and an overlap occurs. The Fermi level crosses the two bands, and the surface becomes metallic. It should be noted that, as usual in the case of surfaces with metallic character, strong atomic rearrangements may occur toward a more stable configuration, which, in this case, is likely to be insulating at zero temperature. However, the search for such a surface configuration was beyond the scope of the present work. As regards the fully defective surface, which represents an epitaxial Mg single layer on top of a MgO(100) surface, its electronic structure results from the partially filled vacancy and surface magnesium bands. This complex

scenario is very far from the naive image of a jellium on top of an insulator, which could still be appropriate for thicker metal-oxide interfaces.

The kinetics of vacancy diffusion on the surface is characterized by a barrier height that was estimated to be equal to about 2 eV. When a diffusing oxygen atom is located at the saddle point, at middistance between two lattice sites, the two excess electron are equally shared between these sites.

ACKNOWLEDGMENTS

We thank C. Henry for his interest and stimulating discussions. The major calculations were performed on the CRAY C98 computer at IDRIS/CNRS, under Project Nos. 970109 and 980732. We are grateful for a generous allocation of time on the machine. The CRMC2 is also associated with the Universities of Aix-Marseille II and III.

*Electronic address: fabio@lps.u-psud.fr

†Electronic address: jacek@crmc2.univ-mrs.fr

‡Electronic address: noguera@lps.u-psud.fr

[1] See, e.g., *Non-Stoichiometric Compounds: Surfaces, Grain Boundaries and Structural Defects*, Vol. 276 of *NATO Advanced Study Institute Series C: Mathematical and Physical Sciences*, edited by J. Nowotny and W. Weppner (Kluwer, Dordrecht, 1989).

[2] V. E. Henrich and P. A. Cox, *The Surface Science of Metal Oxides* (Cambridge University Press, Cambridge, 1994).

[3] C. Noguera, *Physics and Chemistry at Oxide Surfaces* (Cambridge University Press, Cambridge, 1996).

[4] R. Tetot and G. Boureau, Phys. Rev. B **40**, 2311 (1989).

[5] K. C. To, A. M. Stoneham, and B. Henderson, Phys. Rev. **186**, 1237 (1969).

[6] B. Henderson and D. H. Bowen, J. Phys. C **4**, 1487 (1971).

[7] M. C. Wu, C. M. Truong, and D. W. Goodman, Phys. Rev. B **46**, 12 688 (1992).

[8] H. Terauchi and J. B. Cohen, Acta Crystallogr., Sect. A: Cryst. Phys., Diffr., Theor. Gen. Crystallogr. **34**, 556 (1978).

[9] S. Bartkowski, M. Neumann, E. Z. Kurmaev, V. V. Fedorenko, S. N. Shamin, V. M. Cherkashenko, S. N. Nemnonov, A. Winiarski and D. C. Rubie, Phys. Rev. B **56**, 10 656 (1997).

[10] A. Gibson, R. Haydock, and J. P. LaFemina, Phys. Rev. B **50**, 2582 (1994).

[11] Z. R. Dai, Z. L. Wang, and W. X. Liu, Philos. Mag. A **73**, 1685 (1996).

[12] G. A. Ol'khovic, I. I. Naumov, and O. I. Velikokhatnyi, J. Phys.: Condens. Matter **7**, 1273 (1995).

[13] G. Pacchioni, A. M. Ferrari, and G. Ierano, Faraday Discuss. **106**, 155 (1997).

[14] L. N. Kantorovich, J. M. Holender, and M. J. Gillan, Surf. Sci. **343**, 221 (1995).

[15] I. Manassidis, J. Goniakowski, L. N. Kantorovich, and M. J. Gillan, Surf. Sci. **339**, 258 (1995).

[16] C. Noguera, A. Pojani, F. Finocchi and J. Goniakowski, in *Chemisorption and Reactivity on Supported Clusters and Thin Films*, Vol. 331 of *NATO Advanced Study Institute, Series E: Applied Sciences*, edited by R. M. Lambert and G. Pacchioni (Kluwer, Dordrecht, 1997), p. 455.

[17] E. Castanier and C. Noguera, Surf. Sci. **364**, 17 (1996).

[18] P. Zschack, J. B. Cohen, and Y. W. Chung, Surf. Sci. **262**, 395 (1992).

[19] P. J. Hardman, N. S. Prakash, C. A. Muryn, G. N. Raikar, A. G. Thomas, A. F. Prime, G. Thornton, and R. J. Blake, Phys. Rev. B **47**, 16 056 (1993).

[20] P. W. Murray, F. M. Leibsle, C. A. Muryn, H. J. Fischer, C. F. J. Flipse, and G. Thornton, Surf. Sci. **321**, 217 (1994).

[21] P. W. Murray, F. M. Leibsle, C. A. Muryn, H. J. Fisher, C. F. J. Flipse, and G. Thornton, Phys. Rev. Lett. **72**, 689 (1994).

[22] M. Sander and T. Engel, Surf. Sci. Lett. **302**, L263 (1994).

[23] H. Onishi and Y. Iwasawa, Surf. Sci. Lett. **313**, L783 (1994).

[24] D. F. Cox, T. B. Fryberger, and S. Semancik, Surf. Sci. **224**, 121 (1989).

[25] T. Matsumoto, H. Tanaka, T. Kawai, and S. Kawai, Surf. Sci. Lett. **278**, L153 (1992).

[26] Y. Liang and D. A. Bonnell, Surf. Sci. Lett. **285**, L510 (1993).

[27] H. Tanaka, T. Matsumoto, T. Kawai, and S. Kawai, Surf. Sci. **318**, 29 (1994).

[28] C. C. Chang, J. Appl. Phys. **19**, 5570 (1968).

[29] T. M. French and G. A. Somorjai, J. Phys. Chem. **74**, 2489 (1970).

[30] S. Baik, D. E. Fowler, J. M. Blakely, and R. Raj, J. Am. Ceram. Soc. **68**, 281 (1985).

[31] M. Gautier, J. P. Duraud, L. Pham Van, and M. J. Guittet, Surf. Sci. **250**, 71 (1991).

[32] M. Gautier, G. Renaud, L. Pham Van, B. Villette, M. Pollak, N. Thromat, F. Jollet, and J. P. Duraud, J. Am. Ceram. Soc. **77**, 323 (1994).

[33] G. Renaud, B. Villette, I. Vilfan, and A. Bourret, Phys. Rev. Lett. **73**, 1825 (1994).

[34] J. W. He and P. J. Moller, Chem. Phys. Lett. **129**, 13 (1986).

[35] E. Castanier and C. Noguera, Surf. Sci. **364**, 1 (1996).

[36] A. M. Ferrari and G. Pacchioni, J. Phys. Chem. **99**, 17 010 (1995).

[37] E. Scorza, U. Birkenheuer, and C. Pisani, J. Phys. Chem. **107**, 9645 (1997).

[38] A. Gibson, R. Haydock, and J. P. LaFemina, Appl. Surf. Sci. **72**, 285 (1993).

[39] L. Kleinman and D. M. Bylander, Phys. Rev. Lett. **48**, 1425 (1982).

[40] N. Troullier and J. L. Martins, Phys. Rev. B **43**, 1993 (1991).

[41] F. Finocchi and C. Noguera, Phys. Rev. B **53**, 4989 (1996).

[42] S. L. Cunningham, Phys. Rev. B **10**, 4988 (1974).

[43] D. J. Chadi and M. L. Cohen, Phys. Rev. B **8**, 5747 (1973).

[44] M. Methfessel, Phys. Rev. B **38**, 1537 (1988); M. Methfessel, C. O. Rodriguez, and O. K. Andersen, *ibid.* **40**, 2009 (1989); details of the calculation for the perfect MgO(100) surface are given in J. Goniakowski, *ibid.* **57**, 1935 (1998).

[45] O. Robach, G. Renaud, and A. Barbier, Surf. Sci. **401**, 227 (1998).

[46] D. Ferry, J. Suzanne, V. Panella, A. Barbieri, M. A. Van Hove, and J. P. Bibérian, J. Vac. Sci. Technol. (to be published).

[47] The convergence tests were performed on the $n_F = 50\%$ (h) configuration, characterized by the largest dispersion of the vacancy band and no overlap with the conduction band, which thus should suffer from the largest errors. For this configuration, the formation energy (no atomic relaxation) amounts to 10.42 eV when sampling the Brillouin zone corresponding to the $(2\sqrt{2}\times 2\sqrt{2})R45°$ with the Γ point, and to 10.25, 10.28, and 10.29 eV for the $(\sqrt{2}\times\sqrt{2})R45°$ surface unit cell by using one,

three, and ten special **k** points in the irreducible part of the BZ, respectively. We thus take 0.1 eV as an estimation of the BZ sampling-induced error of the calculated formation/interaction energies, and in the following we will give the calculated vacancy formation/interaction energetics with only one-digit precision.

[48] V. Kempter (private communication).

[49] In this calculation, the gap width is equal to 5.5 eV, an underestimated value due to the use of DFT.

[50] R. W. Godby, M. Schlüter, and L. J. Sham, Phys. Rev. B **37**, 10 159 (1988).

[51] F. Didier and J. Jupille, Surf. Sci. **307-309**, 587 (1994).

[52] M. L. Burke and D. W. Goodman, Surf. Sci. **311**, 17 (1994).

[53] Y. Oishi, K. Ando, H. Kurokawa, and Y. Hiro, J. Am. Ceram. Soc. **66**, C60 (1983).

[54] W. Komatsu and Y. Ikuma, in *Proceedings of the 10th International Symposium on the Reactivity of Solids*, edited by P. Barret (Pergamon, Oxford, 1984).

[55] E. A. Kotomin, M. M. Kuklja, R. I. Eglitis, and A. I. Popov, Mater. Sci. Eng. B **37**, 212 (1996).

[56] A. D. Becke, Phys. Rev. A **38**, 3098 (1988); J. P. Perdew, Phys. Rev. B **33**, 8822 (1986).

[57] As shown recently [M. Fuchs *et al.*, Phys. Rev. B **57**, 2134 (1998)], a definite conclusion on this point requires to treating not only valence electrons but also core electrons in the GGA approximation. However, in this system, the core polarization should be very weak.